Zheng et al., http://www.jgp.org/cgi/content/full/jgp.201511448/DC1

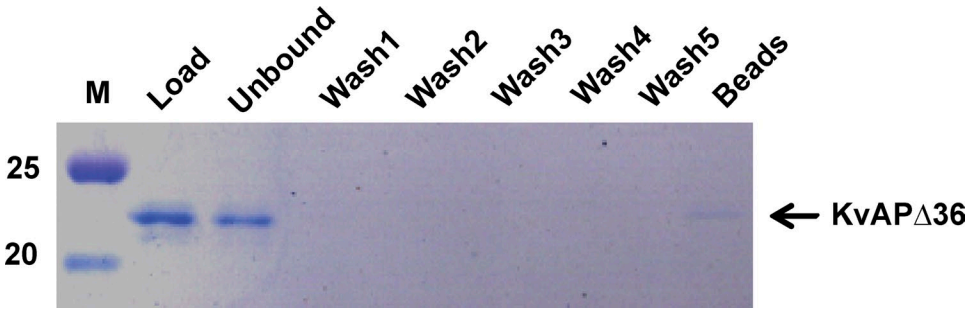

Figure S1. Tracking the channel protein during the preparation of the bSUMs. M, marker; Load, KvAP used for reconstitution; unbound, the supernatant after the pelleting of reconstituted beads; Washes 1–5, the reconstituted beads were washed five times with a buffer containing 150 mM KCl and 10 mM HEPES, pH 7.4. Beads: 20 mM DM and 300 mM imidazole in the washing buffer were used to extract the KvAP protein from the bSUMs. The samples were assayed via Coomassie blue–stained SDS-PAGE. The arrow points to the band of KvAP.

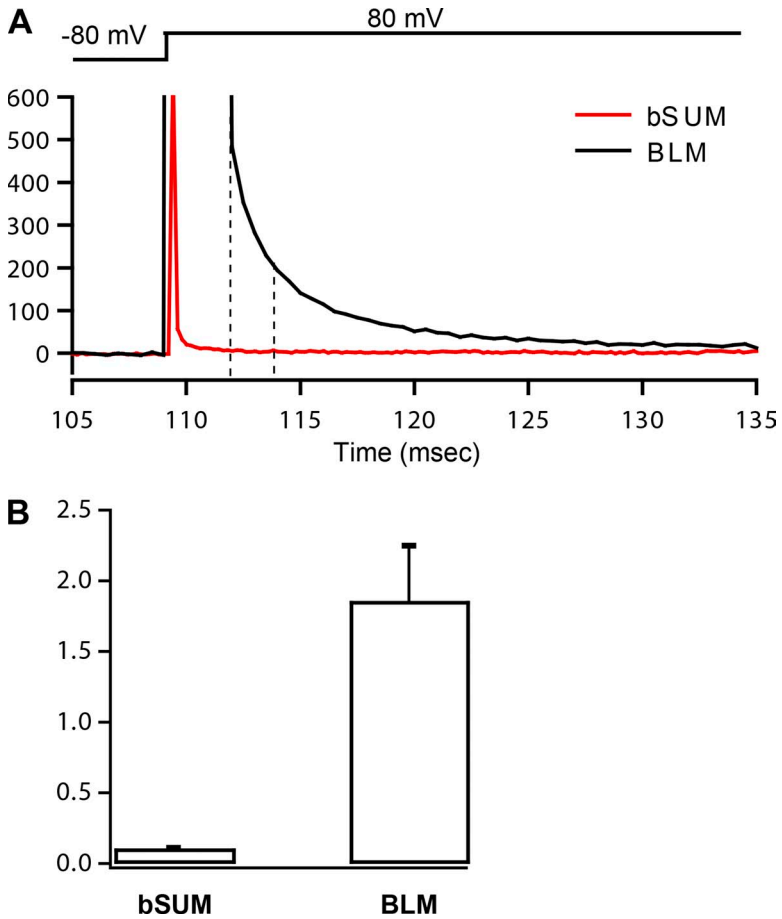

Figure S2. Clamp speed in the patch recordings of a bSUM appears much faster than that of a bilayer lipid membrane (BLM). (A) Current traces from the PE/PG membranes (red from the bSUM and black from the BLM) were triggered by test pulses from −80 to 80 mV. In the cell-attach mode recording of the bSUM, capacitance compensation was tuned. Recordings of the BLM were made with the amplifier set in whole-cell mode. It was difficult to compensate for the BLM capacitance current using our amplifier. The traces were fitted with a single-exponential function, and the resultant time constants were used to estimate clamp speed. (B) Comparison of the kinetic results from various PE/PG membranes. Tau values are 0.11 ± 0.01 ms for the bSUM and 1.9 ± 0.3 ms for the BLM ($n = 3$). The error bars represent standard deviations from three different measurements. The capacitance component of the BLM is ∼20-fold slower than that of the bSUM.

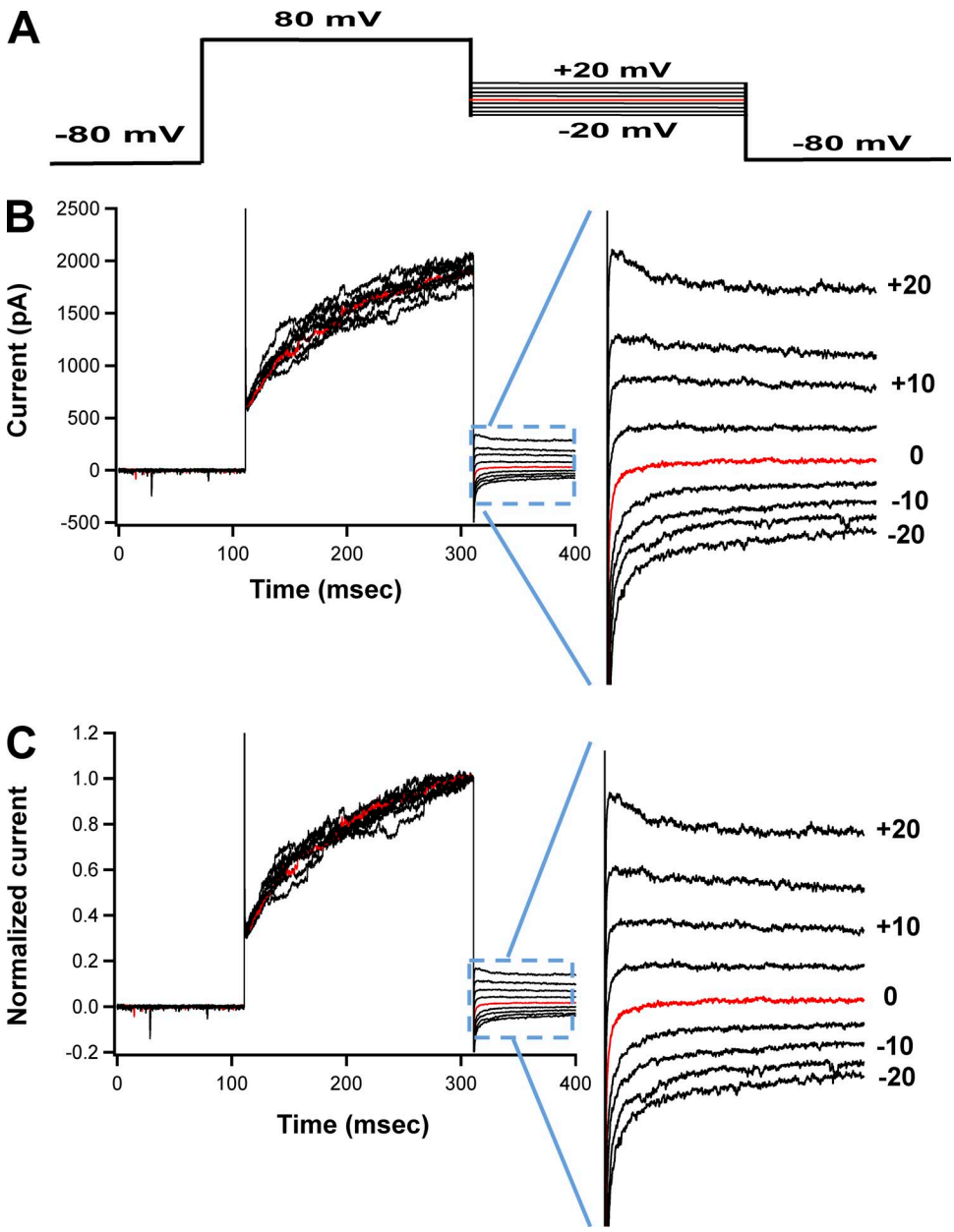

Figure S3. Analysis of tail currents to identify the reversal potential level. (A) The voltage-clamp pulses. The interval between pulses was 60 s, and the tail current segments varied from −20 to 20 mV in 5-mV steps. (B) Probably as a result of the slow kinetics of activation, the currents recorded from the same patch showed variations in the current size during the first 200-ms activation phase of the 80-mV segment. Even so, the tail currents clearly showed the change of ion flow from outward to inward around 0 mV (the red trace), suggesting that the reversal potential is around 0 mV. (C) To minimize the effect of the current variations in the activation segment, each current trace, after leak correction, was normalized against the current at the end of the 200-ms activation at 80 mV. The tail currents before and after normalization were expanded to the right side in both B and C. The normalized currents were plotted as in Fig. 7 D, and a linear fitting of the points around the roughly estimated reversal potential was used to obtain a more accurate value for the measured reversal potential. The solutions used for the experiments had 150 mM KCl in the intracellular side and 90 mM KCl and 60 mM KF in the extracellular side, and the Nernst potential for potassium was 0 mV.